Commun Math Stat (2013) 1:143–162
DOI 10.1007/s40304-013-0012-8

Supercloseness of the Divergence-Free Finite Element Solutions on Rectangular Grids

Yunqing Huang · Shangyou Zhang

Received: 20 April 2013 / Accepted: 20 May 2013 / Published online: 9 July 2013

Abstract By the standard theory, the stable $Q_{k+1,k} - Q_{k,k+1}/Q_k^{dc'}$ divergence-free element converges with the optimal order of approximation for the Stokes equations, but only order k for the velocity in H^1-norm and the pressure in L^2-norm. This is due to one polynomial degree less in y direction for the first component of velocity, which is a $Q_{k+1,k}$ polynomial of x and y. In this manuscript, we will show by supercloseness of the divergence free element that the order of convergence is truly $k+1$, for both velocity and pressure. For special solutions (if the interpolation is also divergence-free), a two-order supercloseness is shown to exist. Numerical tests are provided confirming the accuracy of the theory.

Keywords Mixed finite element · Stokes equations · Divergence-free element · Quadrilateral element · Rectangular grids · Supercloseness · Superconvergence

Mathematics Subject Classification (2010) 65M60 · 65N30 · 76D07

1 Introduction

The divergence-free finite element method is mainly for solving incompressible flow problems, such as Stokes or Navier–Stokes equations, where the finite element space for the pressure is exactly the divergence of the finite element space for the velocity.

Y. Huang
Hunan Key Laboratory for Computation and Simulation in Science and Engineering, Xiangtan University, Xiangtan 411105, China
e-mail: huangyq@xtu.edu.cn

S. Zhang (✉)
Department of Mathematical Sciences, University of Delaware, Newark, DE 19716, USA
e-mail: szhang@udel.edu

In such a method, the finite element velocity is divergence-free pointwise, i.e., the incompressibility condition is enforced strongly. Traditional finite elements enforce the incompressibility weakly, cf. [10, 21]. That is, in order to satisfy the inf-sup stability condition, the incompressibility condition is weakened by either enlarging the velocity space or decreasing the pressure space. This often leads to some sub-optimal methods, or a waste of computation, due to the imperfect matching of two spaces. It may also lead to an inaccurate mass conservation, which is critical in certain computational problems. For example, for a high pressure flow problem, the Taylor–Hood finite element method produces a solution of large error of order $O(Re)$ where Re is the Reynolds number [11].

A fundamental study on the divergence-free element method was done by Scott and Vogelius [22, 23], which shows that the P_{k+1}/P_k^{dc} method is stable (except on grids with nearly-singular vertexes) and consequently of the optimal order on 2D triangular grids, for $k \geq 3$. Here the finite element space for velocity is the space of continuous piecewise-polynomials of degree $(k+1)$ or less; The space approximating pressure is the space of discontinuous piecewise-polynomials of degree k or less, or the divergence of the discrete velocity space, to be precise. There are several other such divergence-free finite elements, cf. [2, 14, 16, 17, 19, 20, 29–31, 33].

Starting from the most popular element, the Q_1/P_0 element [6, 7], there is a series of works on Q_k mixed finite elements on rectangular grids in 2D and 3D. Brezzi and Falk showed that the Q_{k+1}/Q_k^{dc} element is unstable in [9], for any $k \geq 0$. Here Q_k^{dc} denotes the space of discontinuous piecewise-polynomials. In [27], Stenberg and Suri showed the stability, but a sub-optimal order of approximation, for the Q_{k+1}/Q_{k-1}^{dc} element for all $k \geq 1$ in 2D. Bernardi and Maday proved the stability and the optimal order of convergence for the Q_{k+1}/P_k^{dc} element, cf. [4]. Ainsworth and Coggins established [1] the stability and the optimal order of convergence for the Taylor–Hood Q_{k+1}/Q_k element, where the pressure space is continuous too. The Bernardi–Raugel element [5] optimizes the Q_{k+1}/Q_{k-1}^{dc} element, when $k = 1$, by reducing the velocity space to $Q_{1,2} - Q_{2,1}$ polynomials. Here the first component of velocity in the Bernardi–Raugel element is a polynomial of degree 1 in x direction, but of degree 2 in y direction. To be precise, the Bernardi–Raugel element enriches the Q_1 velocity space by face-bubble functions. Similar to the Bernardi–Raugel element, a divergence-free finite element, $Q_{k+1,k} - Q_{k,k+1}/Q_k^{dc'}$ $(k \geq 2)$, was proposed in [31], which further optimizes the Bernardi–Raugel element by increasing the polynomial degree of pressure from $(k-1)$ to k. The nodal degrees of freedom of this divergence-free element and the Bernardi–Raugel element are plotted in Fig. 1. This divergence-free element was extended to its lowest-order form, $k = 1$, i.e., $Q_{2,1} - Q_{1,2}/Q_1^{dc'}$, in [17]. Here the space $Q_k^{dc'}$ for the pressure is the space of discontinuous Q_k polynomials with all spurious modes removed, i.e., eliminating one degree of freedom at each vertex, cf. (2.7). In the construction, the pressure space is exactly the divergence of the velocity. Thus, the resulting finite element is divergence-free pointwise. In such a case, the discrete pressure space can be omitted in the computation. By an iterated penalty method, we obtain the pressure solution as a byproduct, cf. [30] and Sect. 4 below. However, by the standard finite element theory developed in [17, 31], this divergence-free element converges at order k only, due to a degree k polynomial in y for the first component of $\mathbf{u}_h$. This cannot be improved by the standard theory, where the optimal order of convergences is derived from the inf-sup stability.

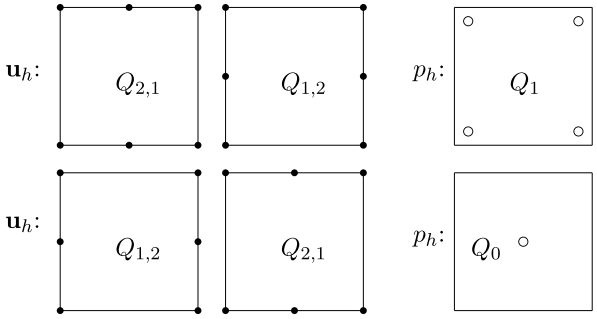

Fig. 1 Nodes of $\mathbf{u}_h/p_h$ for divergence-free (*top*) and Bernardi–Raugel elements

In this manuscript, we further study this $Q_{k+1,k} - Q_{k,k+1}$ divergence-free element and show its supercloseness that the element does converge at order $k+1$. Further the velocity solution of the $Q_{k+1,k} - Q_{k,k+1}$ divergence-free element may be ultraclose, i.e., two orders higher than the standard approximation, provided the interpolation is divergence-free. The extension of this divergence-free element to 3D is straightforward, so is its supercloseness property. By the supercloseness of the finite element solution, traditionally we interpolate the finite element solution by either a $(Q_{k+2})^2$ or a $(Q_{2k})^2$ polynomial piecewise on two by two sub-grids, to obtain a superconvergent solution. It may not be meaningful to do so here as such an interpolation is no longer divergence free. We do get a higher-order solution though, but we lose its mass conservation property. To keep its divergence-free property, we need to post-process this higher-order interpolation. It may cost even more to post-process this interpolated high-order polynomial solution to get a divergence-free solution than to compute directly a higher order divergence-free solution from the family of finite elements.

The divergence-free element is connected to the $C^1 - Q_k$ element [18, 32]. A mathematical interest of this work is its application to the superconvergence analysis of the whole family of $C^1 - Q_k$ elements. We intend to do so in a forthcoming work. Only the superconvergence of the degree-three $C^1 - Q_k$ element, the Bogner–Fox–Schmit element, is established at the moment [18, 26]. We note that such a Q_k-type divergence-free element exists only on rectangular grids, not on general quadrilateral grids. Correspondingly, a construction of $C^1 - Q_k$ elements is not possible yet, on quadrilateral grids.

The rest of the paper is organized as follows. In Sect. 2, we define the finite element for the stationary Stokes equations. In Sect. 3, we establish supercloseness for the divergence-free element. In Sect. 4, we provide some test results confirming the analysis. In particular, we show the order of convergence of the divergence-free element is one higher than that of the rotated Bernardi–Raugel element.

2 The $Q_{k+1,k} - Q_{k,k+1}$ Divergence-Free Element

In this section, we shall define the divergence-free finite element for the stationary Stokes equations on rectangular grids. The resulting finite element solutions for the velocity are divergence-free point wise.

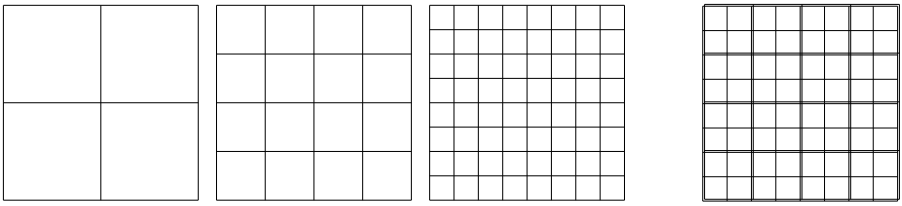

Fig. 2 Three levels of grids, and a macro-element grid (for $k = 1$ only)

We consider a model stationary Stokes problem: Find the velocity $\mathbf{u}$ and the pressure p on a 2D polygonal domain Ω, which can be subdivided into rectangles, such that

$$\begin{aligned} -\Delta \mathbf{u} + \nabla p &= \mathbf{f} \quad \text{in } \Omega, \\ \operatorname{div} \mathbf{u} &= 0 \quad \text{in } \Omega, \\ \mathbf{u} &= \mathbf{0} \quad \text{on } \partial\Omega. \end{aligned} \tag{2.1}$$

The weak form for (2.1) is: Find $\mathbf{u} \in H_0^1(\Omega)^2$ and $p \in L_0^2(\Omega) := L^2(\Omega)/C = \{p \in L^2 \mid \int_\Omega p = 0\}$ such that

$$\begin{aligned} a(\mathbf{u}, \mathbf{v}) + b(\mathbf{v}, p) &= (\mathbf{f}, \mathbf{v}) \quad \forall \mathbf{v} \in H_0^1(\Omega)^2, \\ b(\mathbf{u}, q) &= 0 \quad \forall q \in L_0^2(\Omega). \end{aligned} \tag{2.2}$$

Here $H_0^1(\Omega)^2$ is the subspace of the Sobolev space $H^1(\Omega)^2$ (cf. [13]) with zero boundary trace, and

$$\begin{aligned} a(\mathbf{u}, \mathbf{v}) &= \int_\Omega \nabla \mathbf{u} \cdot \nabla \mathbf{v} \, dx, \\ b(\mathbf{v}, p) &= -\int_\Omega \operatorname{div} \mathbf{v} \, p \, dx, \\ (\mathbf{f}, \mathbf{v}) &= \int_\Omega \mathbf{f}\mathbf{v} \, dx. \end{aligned}$$

The finite element grids are defined by, cf. Fig. 2,

$$\begin{aligned} \mathcal{T}_h = \big\{ K \mid \cup K = \overline{\Omega}, K = [x_a, x_b] \times [y_c, y_d] \text{ with size} \\ h_K = \max\{x_b - x_a, y_d - y_c\} \le h \big\}. \end{aligned}$$

We further assume, only for the lowest-order element $k = 1$ in (2.3), that the rectangles in grid $\mathcal{T}_h$ can be combined into groups of four to form a macro-element grid:

$$\mathcal{M}_h = \left\{ M \mid M = \bigcup_{i=1}^{4} K_i = [x_{i-1}, x_{i+1}] \times [y_{j-1}, y_{j+1}], K_i \in \mathcal{T}_h, \bigcup K_i = \Omega \right\}.$$

See the fourth diagram in Fig. 2. The polynomial spaces are defined by

$$Q_{k,l} = \left\{ \sum_{i \le k, j \le l} c_{ij} x^i y^j \right\}, \qquad Q_k = Q_{k,k}.$$

The $Q_{k+1,k} - Q_{k,k+1}$ $(k \ge 1)$ element spaces are

$$\mathbf{V}_h = \left\{ \mathbf{v}_h \in C(\Omega)^2 \mid \mathbf{v}_h|_K \in Q_{k+1,k} \times Q_{k,k+1} \ \forall K \in \mathcal{T}_h, \text{ and } \mathbf{u}_h|_{\partial\Omega} = 0 \right\}, \tag{2.3}$$

$$P_h = \{ \operatorname{div} \mathbf{u}_h \mid \mathbf{u}_h \in \mathbf{V}_h \}. \tag{2.4}$$

Since $\int_\Omega p_h = \int_\Omega \operatorname{div} \mathbf{u}_h = \int_{\partial\Omega} \mathbf{u}_h = 0$ for any $p_h \in P_h$, we conclude that

$$\mathbf{V}_h \subset H_0^1(\Omega)^2, \qquad P_h \subset L_0^2(\Omega),$$

i.e., the mixed-finite element pair is conforming. The resulting system of finite element equations for (2.2) is: Find $\mathbf{u}_h \in \mathbf{V}_h$ and $p_h \in P_h$ such that

$$\begin{aligned} a(\mathbf{u}_h, \mathbf{v}) + b(\mathbf{v}, p_h) &= (\mathbf{f}, \mathbf{v}) \quad \forall \mathbf{v} \in \mathbf{V}_h, \\ b(\mathbf{u}_h, q) &= 0 \quad \forall q \in P_h. \end{aligned} \tag{2.5}$$

Traditional mixed-finite elements require the inf-sup condition to guarantee the existence of discrete solutions. As (2.4) provides a compatibility between the discrete velocity and the discrete pressure spaces, the linear system of equations (2.5) always has a unique solution, cf. [30]. Furthermore, such a solution $\mathbf{u}_h$ is divergence-free: by the second equation in (2.5) and the definition of P_h in (2.4),

$$b(\mathbf{u}_h, q) = b(\mathbf{u}_h, -\operatorname{div} \mathbf{u}_h) = \| \operatorname{div} \mathbf{u}_h \|^2_{L^2(\Omega)^2} = 0. \tag{2.6}$$

In this case, i.e., $\mathbf{V}_h \subset \mathbf{Z} := \{ \operatorname{div} \mathbf{v} \mid \mathbf{v} \in H_0^1(\Omega)^2 \}$, we call the mixed finite element a divergence-free element. It is apparent that the discrete velocity solution is divergence-free if and only if the discrete pressure finite element space is the divergence of the discrete velocity finite element space, i.e., (2.4).

As singular vertices are present (see [17, 22, 23, 31]), by the definition (2.4), P_h is a subspace of the discontinuous, piecewise Q_k polynomials:

$$P_h = \left\{ p_h \in L_0^2(\Omega) \, | v_h|_K \in Q_k \ \forall K \in \mathcal{T}_h, \sum_{i=1}^{4} (-1)^k p_h|_{K_i}(\mathbf{x}) \ \forall \mathbf{x} \in \mathcal{T}_h \right\}, \tag{2.7}$$

where K_i are four squares numbered counterclockwise around a vertex $\mathbf{x}$ in the grid $\mathcal{T}_h$. It is possible, but very difficult to find a local basis for P_h. But on the other side, it is the special interest of the divergence-free finite element method that the space P_h can be omitted in computation and the discrete solutions approximating the pressure function in the Stokes equations can be obtained as byproducts, if an iterated penalty method is adopted to solve the system (2.5), cf. [8, 10, 15, 25, 30] for more information.

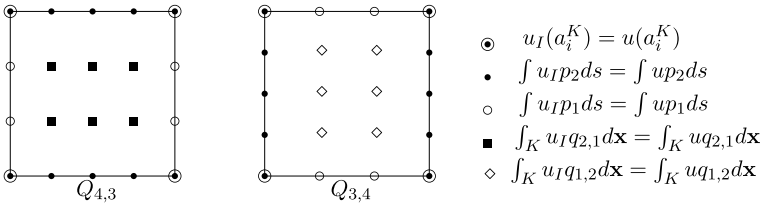

Fig. 3 Three types of interpolation nodes, $k = 3$

3 Supercloseness

As usual, the supercloseness is obtained by the method of integration by parts, cf. [12, 28]. But we have a long series of lemmas dealing with each term in the bilinear forms $a(\cdot,\cdot)$ and $b(\cdot,\cdot)$.

For a convenience in referring components of the vector velocity, we define the two inhomogeneous polynomial spaces:

$$V_{h,1} = \left\{\phi \in H_0^1(\Omega) \mid \phi|_K \in Q_{k+1,k}\ \forall K \in \mathcal{T}_h\right\}, \tag{3.1}$$

$$V_{h,2} = \left\{\phi \in H_0^1(\Omega) \mid \phi|_K \in Q_{k,k+1}\ \forall K \in \mathcal{T}_h\right\}, \tag{3.2}$$

$k \geq 1$. That is,

$$\mathbf{V}_h = V_{h,1} \times V_{h,2}, \quad k \geq 1.$$

The interpolation operator $\mathbf{I}_h$ is defined for the two components of $\mathbf{u}$:

$$\begin{aligned} &\mathbf{I}_h : H_0^1(\Omega)^2 \cap H^2(\Omega)^2 \to V_{h,1} \times V_{h,2}, \\ &\mathbf{I}_h\mathbf{u} = \mathbf{I}_h \begin{pmatrix} u \\ v \end{pmatrix} = \begin{pmatrix} u_I \\ v_I \end{pmatrix}. \end{aligned} \tag{3.3}$$

We define u_I by its values at the Lagrange nodes. For the nodes at vertexes, we could use the Scott–Zhang [24] interpolation, i.e., the nodal value of u_I is an average on an edge, against a dual basis function at the vertex. When u is a P_k polynomial locally, $u_I(a_i^K) = u(a_i^K)$. But for convenience, also because the function u to be interpolated is very smooth in the analysis, we use the nodal value interpolation at vertexes. The nodal values inside an edge, and inside a square, are defined by proper L^2-projections, i.e., by solving the following equations sequentially (see Fig. 3):

$$(u - u_I)\left(a_i^K\right) = 0 \quad \text{at four vertices of } K,\ \forall K \in \mathcal{T}_h, \tag{3.4}$$

$$\int_{y=y_j} (u - u_I)\, p_{k-1}(x)\, dx = 0 \quad \text{on the top and bottom edges of } K, \tag{3.5}$$

$$\int_{x=x_i} (u - u_I)\, p_{k-2}(y)\, dy = 0 \quad \text{on the left and right edges of } K, \tag{3.6}$$

$$\int_K (u - u_I) q_{k-1,k-2}\, d\mathbf{x} = 0 \quad \text{on the square } K, \tag{3.7}$$

where $p_k \in P_k$, the space of 1D polynomials of degree k or less, and $q_{k,l} \in Q_{k,l}$. By rotating x and y, v_I is defined similarly/symmetrically to u_I.

Lemma 3.1 (two-order supercloseness) *For any $Q_{k+1,k}$ function $\psi \in V_{h,1}$, defined in (3.1), for any $u \in H^{k+3}(\Omega) \cap H_0^1(\Omega)$, and for all $k > 1$,*

$$\left| \int_\Omega (u - u_I)_x \psi_x \, d\mathbf{x} \right| \le C h^{k+2} \|u\|_{H^{k+3}} \|\psi\|_{H^1}. \tag{3.8}$$

Proof We first consider the estimation on the reference element $\hat{K} = [-1, 1]^2$. Since $\psi \in Q_{k+1,k}$, we have an exact Taylor expansion:

$$\psi_x(x, y) = \psi_x(x, 0) + y\psi_{xy}(x, 0) + \cdots + \frac{y^{k-1}}{(k-1)!}\psi_{xy^{k-1}}(x, 0) + \frac{y^k}{k!}\psi_{xy^k}(x, 0), \tag{3.9}$$

where $\psi_x(x, 0)$ and all $\psi_{xy^j}(x, 0)$ are P_k polynomials in x only. We will perform the integration by parts repeatedly. First, for the lower order terms in (3.9), we notice that, by the definition of u_I in (3.5) and (3.7),

$$\begin{aligned} &\int_{\hat{K}} (u - u_I)_x y^j \psi_{xy^j}(x, 0) \, d\mathbf{x} \\ &\quad = \int_{-1}^{1} (u - u_I) y^j \psi_{xy^j}(x, 0) \Big|_{x=-1}^{x=1} dy - \int_{\hat{K}} (u - u_I) y^j \psi_{x^2y^j}(x, 0) \, d\mathbf{x} \\ &\quad = 0, \quad \text{when } j = 0, 1, \ldots, k-2. \end{aligned} \tag{3.10}$$

Please be aware that $\psi_{x^2y^j}(x, 0) \in P_{k-1}(x)$ above. Hence, we need to deal with only the last two terms in (3.9).

For the last two terms in (3.9), in order to do integration by parts, we express the polynomials y^{k-1} and y^k by derivatives of another polynomial:

$$s_k(y) = \frac{(y^2-1)^{k+1}}{(2k+2)!} = \frac{y^{2k+2}}{(2k+2)!} - \frac{(k+1)y^{2k}}{(2k+2)!} + \cdots = \frac{y^{2k+2}}{(2k+2)!} + \tilde{p}_{2k}(y), \tag{3.11}$$

$$s_k^{(j)}(\pm 1) = 0, \quad j = 0, 1, \ldots, k, \tag{3.12}$$

$$s_k^{(k+2)}(y) = \frac{1}{k!} y^k + p_{k-2}(y). \tag{3.13}$$

Here $\tilde{p}_{2k}(y)$ and $p_{k-2}(y)$ denote a polynomial of degree $2k$ and $(k-2)$, respectively. We note that, as in (3.10), the integral of $(u - u_I)_x$ against $p_{k-2}(y)$ is zero. Thus, by (3.10), dropping the first $k-1$ terms, we have

$$\begin{aligned} &\int_{\hat{K}} (u - u_I)_x \psi_x(x, y) \, dx \, dy \\ &\quad = \int_{\hat{K}} (u - u_I)_x \left(s_{k-1}^{(k+1)}(y) \psi_{xy^{k-1}}(x, 0) + s_k^{(k+2)}(y) \psi_{xy^k}(x, 0) \right) dx \, dy \end{aligned}$$

$$= \int_{-1}^{1} \left[(u - u_I)_x \left(s_{k-1}^{(k)}(y) \psi_{xy^{k-1}}(x,0) + s_k^{(k+1)}(y) \psi_{xy^k}(x,0) \right) \right]_{y=-1}^{y=1} dx$$

$$- \int_{\hat{K}} (u - u_I)_{xy} \left(s_{k-1}^{(k)}(y) \psi_{xy^{k-1}}(x,0) + s_k^{(k+1)}(y) \psi_{xy^k}(x,0) \right) dx\, dy. \quad (3.14)$$

Let us consider the first boundary integral in (3.14), on the top edge of the square $\hat{K}$. By (3.4) and (3.5),

$$\begin{aligned} &\int_{-1}^{1} (u - u_I)_x(x,1) s_{k-1}^{(k)}(1) \psi_{xy^{k-1}}(x,0)\, dx \\ &= \left[(u - u_I)(x,1) s_{k-1}^{(k)}(1) \psi_{xy^{k-1}}(x,0) \right]_{x=-1}^{1} \\ &\quad - s_{k-1}^{(k)}(1) \int_{-1}^{1} (u - u_I)(x,1) \psi_{x^2 y^{k-1}}(x,0)\, dx \\ &= 0, \end{aligned} \quad (3.15)$$

noting again that $\psi_{x^2 y^{k-1}}(x,0)$ is a P_{k-1} polynomial in x only. The other boundary integral in (3.14) is also 0 as $\psi_{x^2 y^k}(x,0) \in P_{k-1}$ too:

$$\begin{aligned} &\int_{-1}^{1} (u - u_I)_x(x,1) s_k^{(k+1)}(1) \psi_{xy^k}(x,0)\, dx \\ &= \left[(u - u_I)(x,1) s_k^{(k+1)}(1) \psi_{xy^k}(x,0) \right]_{x=-1}^{1} \\ &\quad - s_k^{(k+1)}(1) \int_{-1}^{1} (u - u_I)(x,1) \psi_{x^2 y^k}(x,0)\, dx \\ &= 0. \end{aligned} \quad (3.16)$$

That is, the boundary integrals in (3.14) are all zero. We repeat the integration by parts in this direction, while the boundary terms would be zero by (3.12) and (3.5). Note that in the last case, in (3.15) and (3.16), the boundary terms vanish because of (3.4): $(u - u_I)(\pm 1, \pm 1) = 0$, while they vanish below because of (3.12): $s_{k-1}^{(j)}(\pm 1) = 0$ and $s_k^{(j+1)}(\pm 1) = 0$ for $j < k$. By k times more integration by parts, (3.14) would be

$$\begin{aligned} &\int_{\hat{K}} (u - u_I)_x \psi_x\, dx\, dy \\ &= - \int_{\hat{K}} (u - u_I)_{xy} \left(s_{k-1}^{(k)} \psi_{xy^{k-1}}(x,0) + s_k^{(k+1)} \psi_{xy^k}(x,0) \right) dx\, dy \\ &= \int_{\hat{K}} (u - u_I)_{xy^2} \left(s_{k-1}^{(k-1)} \psi_{xy^{k-1}}(x,0) + s_k^{(k)} \psi_{xy^k}(x,0) \right) dx\, dy \\ &\quad - \int_{-1}^{1} (u - u_I)_{xy}(x,1) \left(s_{k-1}^{(k-1)} \psi_{xy^{k-1}}(x,0) + s_k^{(k)} \psi_{xy^k}(x,0) \right)_{y=-1}^{y=1} dx \end{aligned}$$

$$= \int_{\hat{K}} (u - u_I)_{xy^2} \left(s_{k-1}^{(k-1)} \psi_{xy^{k-1}}(x,0) + s_k^{(k)} \psi_{xy^k}(x,0) \right) dx\, dy$$

$$= (-1)^{k+1} \int_{\hat{K}} (u - u_I)_{xy^{k+1}} \left(s_{k-1} \psi_{xy^{k-1}}(x,0) + s_k' \psi_{xy^k}(x,0) \right) dx\, dy. \quad (3.17)$$

We will perform the integration by parts one last time. But this time, we will treat the two terms in the last integral differently:

$$\int_{\hat{K}} (u - u_I)_{xy^{k+1}} s_{k-1} \psi_{xy^{k-1}}(x,0)\, dx\, dy$$

$$= - \int_{\hat{K}} (u - u_I)_{x^2 y^{k+1}} s_{k-1} \psi_{y^{k-1}}(x,0)\, dx\, dy$$

$$+ \int_{-1}^{1} \left[(u - u_I)_{xy^{k+1}} s_{k-1} \psi_{y^{k-1}}(x,0) \right]_{x=-1}^{x=1} dy,$$

$$\int_{\hat{K}} (u - u_I)_{xy^{k+1}} s_k' \psi_{xy^k}(x,0)\, dx\, dy = - \int_{\hat{K}} (u - u_I)_{xy^{k+2}} s_k \psi_{xy^k}(x,0)\, dx\, dy.$$

For the second integral, the boundary term disappears by the condition (3.12). For the first integral, the boundary integrals will be canceled due to the opposite line integrals (one is from the top limit $x = 1$ and one from the bottom limit $x = -1$ of the integral on the neighboring square) on two sides of a vertical edge $x = x_i$ or due to the boundary condition on ψ:

$$\int_{y_j}^{y_{j+1}} (u - u_I)_{xy^{k+1}} \left(x_i^- \right) s_{k-1}(y) \psi_{y^{k-1}} \left(x_i^-, 0 \right) dy$$

$$- \int_{y_j}^{y_{j+1}} (u - u_I)_{xy^{k+1}} \left(x_i^+ \right) s_{k-1}(y) \psi_{y^{k-1}} \left(x_i^+, 0 \right) dy = 0,$$

$$\int_{y_j}^{y_{j+1}} (u - u_I)_{xy^{k+1}} \left(x_i^\pm \right) s_{k-1}(y) \psi_{y^{k-1}} \left(x_i^\pm, 0 \right) dy = 0, \quad \text{if } \{x_i\} \times [y_j, y_{j+1}] \subset \partial\Omega.$$

We also note that the $(k+1)$st and $(k+2)$nd partial derivatives on u_I above are all zero. Hence, we get (3.8) by summing over the estimation on all rectangles $K \in \mathcal{T}_h$, plus a scaling and the Schwarz inequality,

$$\left| \int_\Omega (u - u_I)_x \psi_x \, d\mathbf{x} \right|$$

$$= \left| \sum_K \int_K (u - u_I)_x \psi_x \, d\mathbf{x} \right| = \left| \sum_K \int_{\hat{K}} (u - u_I)_x \psi_x \, d\mathbf{x} \right|$$

$$= \left| \sum_K (-1)^{k+2} \int_{\hat{K}} (u_{x^2 y^{k+1}} s_{k-1} \psi_{y^{k-1}} + u_{xy^{k+2}} s_k \psi_{xy^k}) \, d\mathbf{x} \right|$$

$$\le \sum_K C |u|_{H^{k+3}(\hat{K})} |\psi|_{H^1(\hat{K})} = C \sum_K h^{k+2} |u|_{H^{k+3}(K)} |\psi|_{H^1(K)}$$

$$\le C h^{k+2} |u|_{H^{k+3}(\Omega)} |\psi|_{H^1(\Omega)}.$$

We note that the semi H^1-norm is needed above to bound $\psi_{y^{k-1}}$, when there is no boundary condition on one element K. But higher order norms are equivalent to semi-H^1 norm on one element, $\|\psi_{xy^k}\|_{L^2(\hat{K})} \le C_k|\psi|_{H^1(\hat{K})}$. Thus $k > 1$ is required. □

In the proof, we can see that the decrease of one degree polynomial in y does not change the super-approximation of $Q_{k+1,k}$ in x direction. After (3.17), if we skip the last step of integration by parts, we would get the following corollary. That is, we avoid $\|\psi_{y^{k-1}}\|_{L^2}$ when $k = 1$ which cannot be bounded by $|\psi|_{H^1}$.

Corollary 3.2 (one-order supercloseness) *For any $Q_{k+1,k}$ function $\psi \in V_{h,1}$, defined in (3.1), for any $u \in H^{k+2}(\Omega)$, and for all $k \ge 1$,*

$$\left|\int_\Omega (u - u_I)_x \psi_x \, d\mathbf{x}\right| \le Ch^{k+1}\|u\|_{H^{k+2}}\|\psi\|_{H^1}. \tag{3.18}$$

Symmetrically, switching x and y in Lemma 3.1, we prove the following lemma.

Lemma 3.3 (two-order supercloseness) *For any $Q_{k,k+1}$ function $\psi \in V_{h,2}$, defined in (3.2), and for any $v \in H^{k+3}(\Omega)$, if $k > 1$,*

$$\left|\int_\Omega (v - v_I)_y \psi_y \, d\mathbf{x}\right| \le Ch^{k+2}\|v\|_{H^{k+3}}\|\psi\|_{H^1}. \tag{3.19}$$

For the same reasons in Corollary 3.2, we get the following corollary from Lemma 3.3.

Corollary 3.4 (one-order supercloseness) *For any $Q_{k,k+1}$ function $\psi \in V_{h,2}$, defined in (3.2), for any $v \in H^{k+2}(\Omega) \cap H_0^1(\Omega)$, and for all $k \ge 1$,*

$$\left|\int_\Omega (v - v_I)_y \psi_y \, d\mathbf{x}\right| \le Ch^{k+1}\|v\|_{H^{k+2}}\|\psi\|_{H^1}. \tag{3.20}$$

Though the interpolation order is $(k+2)$ in the above two lemmas, only the $(k+1)$ order in two corollaries can be achieved in computation, due to the coupling of terms in mixed formulation. We prove the approximation properties in the lower polynomial direction next, i.e., the y-derivative convergence of the first component of velocity. Now, even for $k = 1$, we have a two-order supercloseness.

Lemma 3.5 (two-order supercloseness) *For any $Q_{k+1,k}$ function $\psi \in V_{h,1}$, defined in (3.1), for any $u \in H^{k+3}(\Omega) \cap H_0^1(\Omega)$, and for all $k \ge 1$,*

$$\left|\int_\Omega (u - u_I)_y \psi_y \, d\mathbf{x}\right| \le Ch^{k+2}\|u\|_{H^{k+3}}\|\psi\|_{H^1}. \tag{3.21}$$

Proof Again, we first consider the estimation on the reference element $\hat{K} = [-1, 1]^2$. Since the polynomial degree in y is too low, we do Taylor expansion in x direction,

different from the last lemma:

$$\psi_y(x,y)=\psi_y(0,y)+x\psi_{xy}(0,y)+\cdots+\frac{x^k}{k!}\psi_{x^k y}(0,y)+\frac{x^{k+1}}{(k+1)!}\psi_{x^{k+1}y}(0,y).$$

Again, similar to (3.9), the integral of $(u-u_I)_y$ against x^j terms are zero if $j\le k-1$,

$$\begin{aligned}&\int_{\hat K}(u-u_I)_y x^j\psi_{x^j y}(0,y)\,dx\,dy\\&\quad=\int_{-1}^{1}\big[(u-u_I)x^j\psi_{x^j y}(0,y)\big]_{y=-1}^{y=1}dx-\int_{\hat K}(u-u_I)x^j\psi_{x^j y^2}(0,y)\,dx\,dy\\&\quad=0,\end{aligned}$$

noting that $x^j\psi_{x^j y^2}(0,y)\in Q_{k-1,k-2}$. Using the polynomial function $s_k(x)$ defined in (3.11) we have, cf. (3.14),

$$\begin{aligned}&\int_{\hat K}(u-u_I)_y\psi_y\,dx\,dy\\&\quad=\int_{\hat K}(u-u_I)_y\big(s_k^{(k+2)}(x)\psi_{x^k y}(0,y)+s_{k+1}^{(k+3)}(x)\psi_{x^{k+1}y}(0,y)\big)\,dx\,dy\\&\quad=\int_{-1}^{1}\big[(u-u_I)_y\big(s_k^{(k+1)}(x)\psi_{x^k y}(0,y)+s_{k+1}^{(k+2)}(x)\psi_{x^{k+1}y}(0,y)\big)\big]_{x=-1}^{x=1}dy\\&\qquad-\int_{\hat K}(u-u_I)_{xy}\big(s_k^{(k+1)}(x)\psi_{x^k y}(0,y)+s_{k+1}^{(k+2)}(x)\psi_{x^{k+1}y}(0,y)\big)\,dx\,dy.\end{aligned}$$

Here, for the first time integration by parts, the boundary integral disappeared by (3.4), $(u-u_I)(\pm1,\pm1)=0$. In the next $(k+1)$ times of integration by parts, the boundary integrals on $x=\pm1$ would be zero, directly by the boundary condition (3.12) of $s_k(x)$:

$$\begin{aligned}\int_{\hat K}(u-u_I)_y\psi_y\,dx\,dy=(-1)^{k+2}\int_{\hat K}(u-u_I)_{x^{k+2}y}\big(&s_k\psi_{x^k y}(0,y)\\&+s'_{k+1}\psi_{x^{k+1}y}(0,y)\big)\,dx\,dy.\end{aligned}$$

Thus,

$$\begin{aligned}\left|\int_{\hat K}(u-u_I)_y\psi_y\,dx\,dy\right|&\le C\|u_{x^{k+2}y}\|_{L^2(\hat K)}\|\psi_y\|_{L^2(\hat K)}\\&\le C|u|_{H^{k+3}(\hat K)}\|\psi\|_{H^1(\hat K)}.\end{aligned}$$

The rest of the proof repeats that of Lemma 3.1. □

As for above lemmas and corollaries, we can get the following corollary from Lemma 3.5.

Corollary 3.6 *For any $Q_{k+1,k}$ function $\psi \in V_{h,1}$, defined in (3.1), for any $u \in H^{k+2}(\Omega) \cap H_0^1(\Omega)$, and for all $k \geq 1$,*

$$\left| \int_\Omega (u - u_I)_y \psi_y \, d\mathbf{x} \right| \leq Ch^{k+1} \|u\|_{H^{k+2}} \|\psi\|_{H^1}. \tag{3.22}$$

Corollary 3.7 *For any $Q_{k,k+1}$ function $\psi \in V_{h,2}$, defined in (3.2), and for any $u \in H^{k+3}(\Omega) \cap H_0^1(\Omega)$, and for all $k \geq 1$,*

$$\left| \int_\Omega (u - u_I)_x \psi_x \, d\mathbf{x} \right| \leq Ch^{k+2} \|u\|_{H^{k+3}} \|\psi\|_{H^1}, \tag{3.23}$$

$$\left| \int_\Omega (u - u_I)_x \psi_x \, d\mathbf{x} \right| \leq Ch^{k+1} \|u\|_{H^{k+2}} \|\psi\|_{H^1}. \tag{3.24}$$

Now we study the supercloseness in both bilinear forms.

Lemma 3.8 *For any $(\mathbf{v}_h, q_h) \in \mathbf{V}_h \times P_h$, defined in (2.3) and (2.4), and for any $\mathbf{u} \in H^3(\Omega) \cap H_0^1(\Omega)$,*

$$\left| a(\mathbf{u} - \mathbf{I}_h \mathbf{u}, \mathbf{v}_h) \right| \leq Ch^{k+2} \|\mathbf{u}\|_{H^{k+3}(\Omega)^2} \|\mathbf{v}_h\|_{H^1(\Omega)^2}, \quad k > 1, \tag{3.25}$$

$$\left| a(\mathbf{u} - \mathbf{I}_h \mathbf{u}, \mathbf{v}_h) \right| \leq Ch^{k+1} \|\mathbf{u}\|_{H^{k+2}(\Omega)^2} \|\mathbf{v}_h\|_{H^1(\Omega)^2}, \quad k \geq 1, \tag{3.26}$$

$$\left| b(\mathbf{u} - \mathbf{I}_h \mathbf{u}, q_h) \right| \leq Ch^{k+1} \|\mathbf{u}\|_{H^{k+2}(\Omega)^2} \|q_h\|_{L^2(\Omega)}, \quad k \geq 1, \tag{3.27}$$

where $\mathbf{I}_h \mathbf{u}$ is the interpolation of $\mathbf{u}$ defined by (3.3).

Proof (3.25) is a combination of (3.8), (3.21), (3.23), and (3.19). (3.26) is a combination of (3.18), (3.22), (3.24), and (3.20).

For (3.27), we will lose one order of convergence. Let $q_h = \operatorname{div} \mathbf{w}_h$ for some $\mathbf{w}_h = (\phi, \psi) \in \mathbf{V}_h$. We have, denoting $\mathbf{u} = (u, v)$,

$$b(\mathbf{u} - \mathbf{I}_h \mathbf{u}, q_h) = \sum_K \int_K \big((u - u_I)_x + (v - v_I)_y \big) (\phi_x + \psi_y) \, d\mathbf{x}.$$

Here we have two old integrals, $\int_K (u - u_I)_x \phi_x \, d\mathbf{x}$ and $\int_K (v - v_I)_y \psi_y \, d\mathbf{x}$, and two new integrals, $\int_K (u - u_I)_x \psi_y \, d\mathbf{x}$ and $\int_K (v - v_I)_y \phi_x \, d\mathbf{x}$. The approximation order can be one order higher for the two old integrals. For the two new integrals, by symmetry, we consider $\int_K (u - u_I)_x \psi_y \, d\mathbf{x}$. We use the following Taylor expansion on the reference element $\hat{K}$ in the y direction. We note that the Taylor expansion in x direction would lead to a too high order polynomial in y direction each term in (3.28) below:

$$\psi_y(x, y) = \psi_y(x, 0) + y\psi_{y^2}(x, 0) + \cdots + \frac{y^{k-1}}{(k-1)!} \psi_{y^k}(x, 0) + \frac{y^k}{k!} \psi_{y^{k+1}}(x, 0). \tag{3.28}$$

Here all $\psi_{y^j}(x,0)$ are polynomials of degree k in x. That is, a generic term $y^j\psi_{y^{j+1}}(x,0) \in Q_{k,j}$. This is the same as the generic term $y^j\psi_{xy^j}(x,0)$ in the early Taylor expansion (3.9). Thus repeating the proof of Lemma 3.1, we get

$$\int_{\hat{K}} (u-u_I)_x \psi_y \, d\mathbf{x} = \int_{\hat{K}} (u-u_I)_x \big(s_{k-1}^{(k+1)} \psi_{y^k}(x,0) + s_k^{(k+2)} \psi_{y^{k+1}}(x,0)\big)\, dx\, dy$$
$$= (-1)^{k+1} \int_{\hat{K}} u_{xy^{k+1}} \big(s_{k-1}\psi_{y^k}(x,0) + s_k' \psi_{y^{k+1}}(x,0)\big)\, dx\, dy.$$

For the second integral, we can do an integration by parts to raise one more order. But we are limited by the first integral above to get only

$$\left| \int_{\hat{K}} (u-u_I)_x \psi_y \, d\mathbf{x} \right| \le \|u\|_{H^{k+2}(\hat{K})} \|\psi\|_{H^1(\hat{K})}.$$

Similarly, we have the same bound for $|\int_{\hat{K}} (u-u_I)_y \psi_x \, d\mathbf{x}|$. (3.27) follows by the Schwarz inequality and the scaling of referencing mappings. □

Finally, we estimate the approximation to p.

Lemma 3.9 *For any function $\mathbf{v}_h \in \mathbf{V}_h$, defined in (2.3), and for any $p \in H^{k+1}(\Omega) \cap L_0^2(\Omega)$,*

$$\left| \int_\Omega \operatorname{div} \mathbf{v}_h (p - p_I)\, d\mathbf{x} \right| \le C h^{k+1} \|\mathbf{v}_h\|_{H^1} \|p\|_{H^{k+1}}, \tag{3.29}$$

where p_I is a special nodal interpolation of p in P_h, defined in (3.30) below.

Proof We note that P_h are discontinuous Q_k functions, $P_h = \operatorname{div} \mathbf{V}_h$. We define an interpolation operator for P_h via that $\mathbf{I}_h$ for $\mathbf{V}_h$ defined in (3.3). For a $p \in H^2(\Omega) \cap L_0^2(\Omega)$, Arnold, Scott and Vogelius have shown in [3] that there is a $\mathbf{w} \in H^3(\Omega)^2 \cap H_0^1(\Omega)^2$, such that

$$\operatorname{div} \mathbf{w} = p \quad \text{and} \quad \|\mathbf{w}\|_{H^3} \le C \|p\|_{H^2}.$$

For simplicity, we assume the above lifting exists up to order $k+1$. We define

$$p_I = \operatorname{div} \mathbf{w}_I, \tag{3.30}$$

for $\mathbf{w}_I = \mathbf{I}_h \mathbf{w}$ defined by (3.3). In order to use (3.27), we use the notations

$$\mathbf{w} = \begin{pmatrix} u \\ v \end{pmatrix}, \qquad \mathbf{w}_I = \begin{pmatrix} u_I \\ v_I \end{pmatrix}, \qquad \mathbf{v}_h = \begin{pmatrix} \phi \\ \psi \end{pmatrix}.$$

Repeating the proof in Lemma 3.8, we get

$$\begin{aligned}\left|\int_\Omega \operatorname{div}\mathbf{v}_h(p-p_I)\,d\mathbf{x}\right| &= \left|\int_\Omega \operatorname{div}\mathbf{v}_h \operatorname{div}(\mathbf{w}-\mathbf{w}_I)\,d\mathbf{x}\right| \\ &= \left|\int_\Omega \big((u-u_I)_x+(v-v_I)_y\big)(\phi_x+\psi_y)\,d\mathbf{x}\right| \\ &\le Ch^{k+1}\left|\begin{pmatrix}u\\v\end{pmatrix}\right|_{H^{k+2}}\left|\begin{pmatrix}\phi\\\psi\end{pmatrix}\right|_{H^1} \\ &\le Ch^{k+1}\|p\|_{H^{k+1}}\|\mathbf{v}_h\|_{H^1}.\end{aligned}$$

□

We derive the main theorem.

Theorem 3.10 *The finite element solution* $(\mathbf{u}_h, p_h)$ *of* (2.5) *has the following supercloseness property, one order higher than the optimal order,*

$$\|\mathbf{u}_h-\mathbf{I}_h\mathbf{u}\|_{H^1}+\|p_h-p_I\|_{L^2}\le Ch^{k+1}\big(\|\mathbf{u}\|_{H^{k+2}}+\|p\|_{H^{k+1}}\big), \tag{3.31}$$

where the interpolations $(\mathbf{I}_h\mathbf{u}, p_I)$ *are defined in* (3.3) *and* (3.30).

Proof By the inf-sup condition shown in [17, 31], it follows that, cf. [21], for all $(\mathbf{w}_h, r_h)\in\mathbf{V}_h\times P_h$,

$$\sup_{(\mathbf{v}_h,q_h)\in\mathbf{V}_h\times P_h}\frac{a(\mathbf{w}_h,\mathbf{v}_h)+b(\mathbf{v}_h,r_h)+b(\mathbf{w}_h,q_h)}{\|\mathbf{v}_h\|_{H^1}+\|q_h\|_{L^2}}\ge C\big(\|\mathbf{w}_h\|_{H^1}+\|r_h\|_{L^2}\big). \tag{3.32}$$

By Corollary 3.7 and Lemma 3.9, we have

$$\begin{aligned}&\|\mathbf{u}_h-\mathbf{I}_h\mathbf{u}\|_{H^1}+\|p_h-p_I\|_{L^2} \\ &\le C\sup_{(\mathbf{v}_h,q_h)\in\mathbf{V}_h\times P_h}\frac{a(\mathbf{u}_h-\mathbf{I}_h\mathbf{u},\mathbf{v}_h)+b(\mathbf{v}_h,p_h-p_I)+b(\mathbf{u}_h-\mathbf{I}_h\mathbf{u},q_h)}{\|\mathbf{v}_h\|_{H^1}+\|q_h\|_{L^2}} \\ &= C\sup_{(\mathbf{v}_h,q_h)\in\mathbf{V}_h\times P_h}\frac{a(\mathbf{u}-\mathbf{I}_h\mathbf{u},\mathbf{v}_h)+b(\mathbf{v}_h,p-p_I)+b(\mathbf{u}-\mathbf{I}_h\mathbf{u},q_h)}{\|\mathbf{v}_h\|_{H^1}+\|q_h\|_{L^2}} \\ &\le Ch^{k+1}\big(\|\mathbf{u}\|_{H^{k+2}}+\|p\|_{H^{k+1}}\big).\end{aligned}$$

Note that, due to the pointwise divergence free property, above we have

$$b(\mathbf{u}_h-\mathbf{I}_h\mathbf{u},q_h)=b(-\mathbf{I}_h\mathbf{u},q_h)=b(\mathbf{u}-\mathbf{I}_h\mathbf{u},q_h).$$

□

Here, to be precise, we do not have a supercloseness for p in Theorem 3.10. As P_h are degree-k polynomials, the best order approximation to p in L^2-norm would be $(k+1)$. However, due to the mixed formulation, the convergence of p_h to p is limited to the optimal order convergence of $\mathbf{u}_h$, which is $(k-1)$ in H^1-norm as $\mathbf{u}_h$ has polynomial degree k only in y direction for its first component. In this sense, the supercloseness result (3.31) does lift the order of approximation of p_h by one.

For $k > 1$, we may have a two-order supercloseness for the velocity. Such numerical examples are shown in [31] and in next section. That is, for some special functions $\mathbf{u}$, $\mathbf{I}_h\mathbf{u}$ might be also in the divergence-free subspace of $\mathbf{V}_h$. If so, we have a two-order supercloseness result.

Theorem 3.11 (two-order supercloseness) *For some solution* $\mathbf{u}$ *of* (2.1), *if*

$$\mathbf{I}_h\mathbf{u} \in \mathbf{Z}_h := \{\mathbf{z}_h \in \mathbf{V}_h \mid \operatorname{div} \mathbf{z}_h = 0\},$$

where $\mathbf{I}_h$ *is defined in* (3.3), *and if* $k > 1$, *then*

$$\|\mathbf{u}_h - \mathbf{I}_h\mathbf{u}\|_{H^1} \le Ch^{k+2}\|\mathbf{u}\|_{H^{k+3}}. \tag{3.33}$$

Proof By (3.25), limited to the divergence-free subspace,

$$\begin{aligned}\|\mathbf{u}_h - \mathbf{I}_h\mathbf{u}\|_{H^1} &\le \sup_{\mathbf{w}_h\in\mathbf{Z}_h} \frac{a(\mathbf{u}_h - \mathbf{I}_h\mathbf{u}, \mathbf{w}_h)}{\|\mathbf{w}_h\|_{H^1}} \\ &= \sup_{\mathbf{w}_h\in\mathbf{Z}_h} \frac{a(\mathbf{u} - \mathbf{I}_h\mathbf{u}, \mathbf{w}_h)}{\|\mathbf{w}_h\|_{H^1}} \le Ch^{k+2}\|\mathbf{u}\|_{H^{k+3}}.\end{aligned}$$

□

4 Numerical Tests

In this section, we report some results of numerical experiments on the $Q_{k+1,k} - Q_{k,k+1}$ element for the stationary Stokes equations (2.1) on the unit square $\Omega = [0, 1]^2$. The grids $\mathcal{T}_h$ are depicted in Fig. 2, i.e., each squares are refined into four sub-squares each level. The initial grid, level one grid, is simply the unit square.

We choose an exact solution for the Stokes equations (2.1):

$$\mathbf{u} = \mathbf{curl}\, g, \quad p = \Delta g. \tag{4.1}$$

Here

$$g = 2^8\big(x^3 - x^4\big)^2\big(y^3 - y^4\big)^2.$$

So we can compute the right hand side function $\mathbf{f}$ for (2.1) as

$$\mathbf{f} = -\Delta\, \mathbf{curl}\, g + \nabla\Delta g. \tag{4.2}$$

We note that, unlike [17, 31], we intentionally choose a non-symmetric solution so that no ultraconvergence would happen, which does not exist in general. The solution p is plotted in Fig. 4.

We compute the Stokes solution on refined grids, cf. Fig. 2, by the divergence $Q_{k+1,k} - Q_{k,k+1}$ element (2.3) and by the rotated Bernardi–Raugel element [5, 10, 21]:

$$\begin{aligned}\mathbf{V}_h^{\mathrm{BR}} &= \big\{\mathbf{v}_h \in C(\Omega)^2 \cap H_0^1(\Omega)^2 \mid \mathbf{v}_h|_K \in Q_{k+1,k} \times Q_{k,k+1}\ \forall K \in \mathcal{T}_h\big\}, \\ P_h^{\mathrm{BR}} &= \big\{q_h \in L_0^2(\Omega) \mid q_h|_K \in Q_{k-1}\big\}.\end{aligned} \tag{4.3}$$

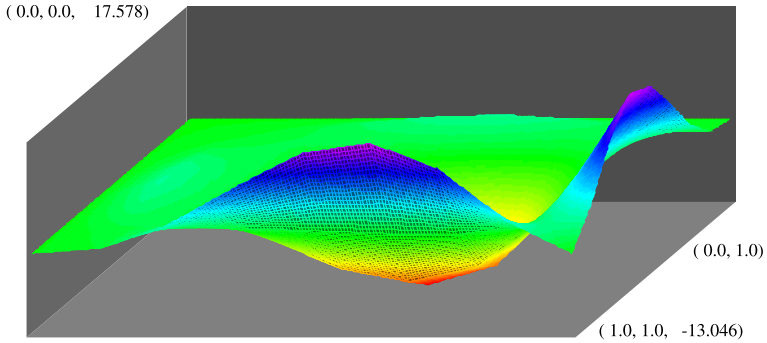

Fig. 4 The solution p (the errors are shown in Fig. 5)

Table 1 The errors $\mathbf{e}_h = \mathbf{I}_h\mathbf{u} - \mathbf{u}_h$ and $\epsilon_h = p_I - p_h$ (one-order supercloseness) for (4.1) with $k = 1$

	$\lvert\mathbf{e}_h\rvert_{L^2}$	h^n	$\lvert\mathbf{e}_h\rvert_{H^1}$	h^n	$\lVert\epsilon_h\rVert_{L^2}$	h^n	
	$Q_{k+1,k} - Q_{k,k+1}$ div-free element (2.3), $k = 1$						#it
2	0.264345		1.341770		5.965379		4
3	0.102329	1.4	0.795594	0.8	1.896372	1.7	4
4	0.026839	1.9	0.219469	1.9	0.481076	2.0	3
5	0.006773	2.0	0.055901	2.0	0.120363	2.0	3
6	0.001697	2.0	0.014035	2.0	0.030083	2.0	3
7	0.000424	2.0	0.003512	2.0	0.007520	2.0	3
	rotated Bernardi–Raugel element (4.3), $k = 1$						#Uz
2	0.570990		3.531380		7.497615		29
3	0.244967	1.2	3.028368	0.2	6.943183	0.1	65
4	0.074335	1.7	1.797533	0.8	3.300598	1.1	136
5	0.019849	1.9	0.946426	0.9	1.575390	1.1	297
6	0.005080	2.0	0.481087	1.0	0.762341	1.0	330
7	0.001281	2.0	0.241916	1.0	0.373990	1.0	204

Following the analysis in [17], the stability of the rotated Bernardi–Raugel element would be proved. For the rotated Bernardi–Raugel element, the system of finite element equations is solved by the Uzawa iterative method, cf. [10, 15, 21]. The stop criterion is the difference $|p_h^{(n)} - p_h^{(n-1)}| \leq 10^{-6}$. We list the number of Uzawa iterations in the data tables by #Uz. Here the interpolation operators are standard Lagrange nodal interpolations [13].

For the $Q_{k+1,k} - Q_{k,k+1}$ divergence-free element, the pressure does not enter into computation, but is obtained as a byproduct, because $P_h = \operatorname{div} \mathbf{V}_h$. The resulting linear system of $Q_{k+1,k} - Q_{k,k+1}$ divergence-free element equations can be formulated as symmetric positive definite. Then the iterated penalty method [15, 31] can be applied to obtain the divergence-free finite element solution for the velocity, and a

Table 2 The errors $\mathbf{e}_h = \mathbf{I}_h\mathbf{u} - \mathbf{u}_h$ and $\epsilon_h = p_I - p_h$ (one-order supercloseness) for (4.1) with $k = 2$

	$\lvert\mathbf{e}_h\rvert_{L^2}$	h^n	$\lvert\mathbf{e}_h\rvert_{H^1}$	h^n	$\lVert\epsilon_h\rVert_{L^2}$	h^n	
	$Q_{k+1,k} - Q_{k,k+1}$ div-free element (2.3), $k = 2$						#it
1	0.322530	0.0	1.580066	0.0	3.546405	0.0	3
2	0.071851	2.2	0.699614	1.2	1.010498	1.8	4
3	0.005510	3.7	0.089611	3.0	0.131816	2.9	3
4	0.000355	4.0	0.010471	3.1	0.015587	3.1	3
5	0.000022	4.0	0.001280	3.0	0.001904	3.0	3
6	0.000001	4.0	0.000159	3.0	0.000236	3.0	3
7	0.000000	4.0	0.000020	3.0	0.000029	3.0	3
	rotated Bernardi–Raugel element (4.3), $k = 2$						#Uz
1	0.645475	0.0	4.250791	0.0	1.143688	0.0	27
2	0.191342	1.8	2.518701	0.8	5.499136	—	67
3	0.025892	2.9	0.673622	1.9	1.621194	1.8	100
4	0.003307	3.0	0.172036	2.0	0.441596	1.9	156
5	0.000419	3.0	0.043543	2.0	0.113029	2.0	266
6	0.000053	3.0	0.010954	2.0	0.028424	2.0	130
7	0.000007	3.0	0.002747	2.0	0.007117	2.0	101

Table 3 The errors $\mathbf{e}_h = \mathbf{I}_h\mathbf{u} - \mathbf{u}_h$ and $\epsilon_h = p_I - p_h$ (one-order supercloseness) for (4.1) with $k = 3$

	$\lvert\mathbf{e}_h\rvert_{L^2}$	h^n	$\lvert\mathbf{e}_h\rvert_{H^1}$	h^n	$\lVert\epsilon_h\rVert_{L^2}$	h^n	
	$Q_{k+1,k} - Q_{k,k+1}$ div-free element (2.3), $k = 3$						#it
1	0.123142	0.0	1.128619	0.0	1.642992	0.0	4
2	0.004515	4.8	0.065512	4.1	0.128938	3.7	3
3	0.000147	4.9	0.003911	4.1	0.008007	4.0	3
4	0.000004	5.0	0.000234	4.1	0.000494	4.0	3
5	0.000000	5.0	0.000014	4.0	0.000031	4.0	3
	rotated Bernardi–Raugel element (4.3), $k = 3$						#Uz
1	0.374364	0.0	3.512050	0.0	6.061521	0.0	57
2	0.021063	4.2	0.375407	3.2	0.736746	3.0	76
3	0.001597	3.7	0.058926	2.7	0.117000	2.7	123
4	0.000111	3.8	0.008169	2.9	0.013672	3.1	177
5	0.000007	3.9	0.001065	2.9	0.001666	3.0	102

byproduct $p_h = \operatorname{div}\mathbf{w}_h$ for the pressure. In our computation, the iterated penalty parameter is 2000. The stop criterion is the divergence $\|\operatorname{div}\mathbf{u}_h^{(n)}\|_0 \le 10^{-9}$. The number of iterated penalty iterations is also listed as #it in the data tables.

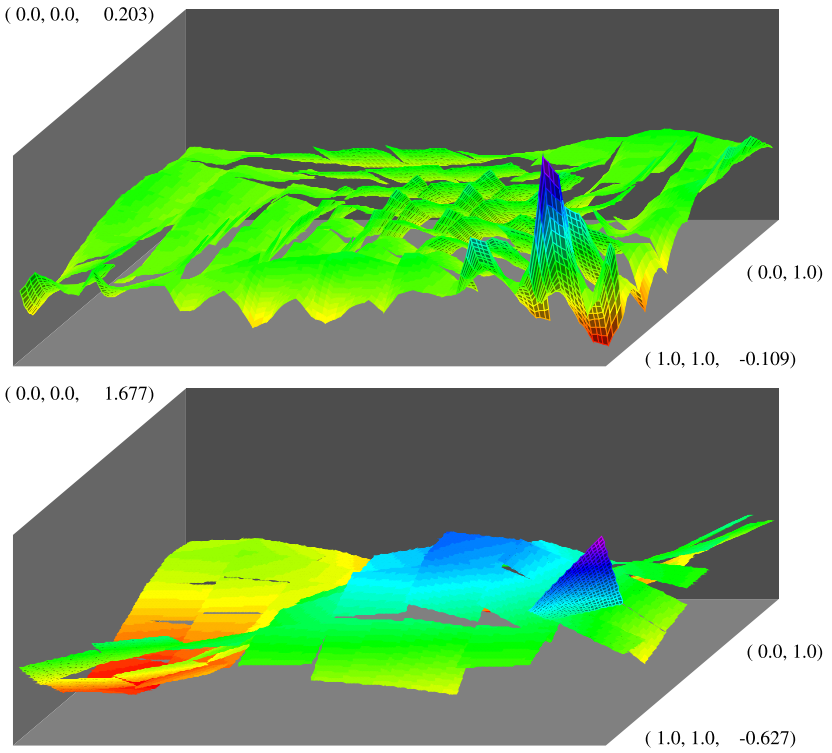

Fig. 5 The errors of p_h for the divergence-free (*top*) and BR elements

In Table 1, we list the errors in various norms for the $Q_{k+1,k} - Q_{k,k+1}$ divergence-free element and for the rotated Bernardi–Raugel element, for $k = 1$. It is clear that the order of convergence is 2, one order higher than that of latter. We note that the convergence order is only 2 for $Q_{2,1} - Q_{1,2}$ divergence-free elements in L^2-norm, i.e., there is no L^2-supercloseness. But we do see L^2-supercloseness for $k > 1$ next.

In Table 2, we list the computation results for $k = 2$ elements. Again, the divergence-free element is one order higher than the rotated Bernardi–Raugel element. To show the difference in the two elements, we plot the errors by two elements on level 4 grid in Fig. 5. One can see the advantage of the divergence-free element, which fully utilizes the approximation power of $\mathbf{u}_h$ by lifting the pressure polynomial degree. Of course, another advantage is the divergence-free solution after such a lift. We next report the results for $k = 3$ in Table 3. All numerical results confirm the theory, and also show the accuracy of the supercloseness analysis.

Finally, we test the two-order supercloseness in Theorem 3.11. We choose a symmetric function as the exact solution of the Stokes equations (2.1):

$$\mathbf{u} = \mathbf{curl}\, g, \quad g = 2^8\big(x - x^2\big)^2\big(y - y^2\big)^2. \tag{4.4}$$

Comparing to the data in Table 3, we can see, in Table 4, that the velocity does converge with another order higher than the optimal order. This is predicted in (3.33).

Table 4 The errors $\mathbf{e}_h = \mathbf{I}_h\mathbf{u} - \mathbf{u}_h$ and $\epsilon_h = p_I - p_h$ (two-order supercloseness) for (4.4) with $k = 3$

	$\lvert\mathbf{e}_h\rvert_{L^2}$	h^n	$\lvert\mathbf{e}_h\rvert_{H^1}$	h^n	$\lVert\epsilon_h\rVert_{L^2}$	h^n	
	$Q_{k+1,k} - Q_{k,k+1}$ div-free element (2.3), $k = 3$(!)						#it
2	0.001196745		0.024927233		0.1147364	3.8	4
3	0.000045519	4.7	0.001383336	4.2	0.0069166	4.1	4
4	0.000000937	5.6	0.000051730	4.7	0.0004383	4.0	4
5	0.000000016	5.8	0.000001826	4.9	0.0000276	4.0	4
6	0.000000000	5.9	0.000000060	4.9	0.0000017	4.0	4

Here the order of convergence for the pressure is the same as that in Table 3. It indicates that the analysis in Theorem 3.10 is sharp. Here we have a two-order supercloseness in L^2-norm too, for the velocity. But the supercloseness in L^2-norm is not studied in this manuscript.

Acknowledgements This research is supported in part by Hunan Key Laboratory for Computation and Simulation in Science and Engineering, Xiangtan University.

References

1. Ainsworth, M., Coggins, P.: A uniformly stable family of mixed hp-finite elements with continuous pressures for incompressible flow. IMA J. Numer. Anal. **22**, 307–327 (2002)
2. Arnold, D.N., Qin, J.: Quadratic velocity/linear pressure Stokes elements. In: Vichnevetsky, R., Steplemen, R.S. (eds.) Advances in Computer Methods for Partial Differential Equations VII (1992)
3. Arnold, D., Scott, L.R., Vogelius, M.: Regular inversion of the divergence operator with Dirichlet conditions on a polygon. Ann. Sc. Norm. Super Pisa, Cl. Sci. **15**, 169–192 (1988)
4. Bernardi, C., Maday, Y.: Uniform inf-sup conditions for the spectral discretization of the Stokes problem. Math. Methods Appl. Sci. **9**, 395–414 (1999)
5. Bernardi, C., Raugel, B.: Analysis of some finite elements of the Stokes problem. Math. Comput. **44**, 71–79 (1985)
6. Boland, J.M., Nicolaides, R.A.: Stability of finite elements under divergence constraints. SIAM J. Numer. Anal. **20**, 722–731 (1983)
7. Boland, J.M., Nicolaides, R.A.: Stable and semistable low order finite elements for viscous flows. SIAM J. Numer. Anal. **22**, 474–492 (1985)
8. Brenner, S.C., Scott, L.R.: The Mathematical Theory of Finite Element Methods. Springer, New York (1994)
9. Brezzi, F., Falk, R.: Stability of higher-order Hood–Taylor methods. SIAM J. Numer. Anal. **28**(3), 581–590 (1991)
10. Brezzi, F., Fortin, M.: Mixed and Hybrid Finite Element Methods. Springer, Berlin (1991)
11. Case, M., Ervin, V., Linke, A., Rebholz, L.: Improving mass conservation in FE approximations of the NSE with C0 velocities: a connection between Scott–Vogelius elements and grad-div stabilization. SIAM J. Numer. Anal. **49**(4), 1461–1481 (2011)
12. Chen, C.M., Huang, Y.Q.: High Accuracy Theory of Finite Element Methods. Hunan Science Press, Hunan (1995) (in Chinese)
13. Ciarlet, P.G.: The Finite Element Method for Elliptic Problems. North-Holland, Amsterdam (1978)
14. Falk, R.S., Neilan, M.: Stokes complexes and the construction of stable finite elements with pointwise mass conservation. SIAM J. Numer. Anal. **51**(2), 1308–1326 (2013)
15. Fortin, M., Glowinski, R.: Augmented Lagrangian Methods: Applications to the Numerical Solution of Boundary-Value Problems. North Holland, Amsterdam (1983)
16. Guzman, J., Neilan, M.: Conforming and divergence-free Stokes elements on general triangular meshes. Math. Comput. (accepted)

17. Huang, Y., Zhang, S.: A lowest order divergence-free finite element on rectangular grids. Front. Math. China **6**(2), 253–270 (2011)
18. Lin, J., Lin, Q.: Superconvergence for the Bogner–Fox–Schmit element. Math. Numer. Sin. **26**(1), 47–50 (2004)
19. Qin, J.: On the convergence of some low order mixed finite elements for incompressible fluids. Thesis, Pennsylvania State University (1994)
20. Qin, J., Zhang, S.: Stability and approximability of the P1-P0 element for Stokes equations. Int. J. Numer. Methods Fluids **54**, 497–515 (2007)
21. Raviart, P.A., Girault, V.: Finite Element Methods for Navier–Stokes Equations. Springer, Berlin (1986)
22. Scott, L.R., Vogelius, M.: Norm estimates for a maximal right inverse of the divergence operator in spaces of piecewise polynomials. RAIRO. Model. Math. Anal. Numer. **19**, 111–143 (1985)
23. Scott, L.R., Vogelius, M.: Conforming finite element methods for incompressible and nearly incompressible continua. In: Lectures in Applied Mathematics, vol. 22, pp. 221–244 (1985)
24. Scott, L.R., Zhang, S.: Finite-element interpolation of non-smooth functions satisfying boundary conditions. Math. Comput. **54**, 483–493 (1990)
25. Scott, L.R., Zhang, S.: Multilevel iterated penalty method for mixed elements. In: The Proceedings for the Ninth International Conference on Domain Decomposition Methods, Bergen, pp. 133–139 (1998)
26. Shu, S., Yu, H., Huang, Y.: Superconvergence and high accuracy combination formula of bicubic spline element for plate problems. Numer. Math. Sin. **20**(2), 167–174 (1998), in Chinese
27. Stenberg, R., Suri, M.: Mixed hp finite element methods for problems in elasticity and Stokes flow. Numer. Math. **72**, 367–389 (1996)
28. Yan, N.: Superconvergence Analysis and a Posteriori Error Estimation in Finite Element Methods. Science Press, Beijing (2008)
29. Zhang, S.: A new family of stable mixed finite elements for 3D Stokes equations. Math. Comput. **74**(250), 543–554 (2005)
30. Zhang, S.: On the P1 Powell–Sabin divergence-free finite element for the Stokes equations. J. Comput. Math. **26**, 456–470 (2008)
31. Zhang, S.: A family of $Q_{k+1,k} \times Q_{k,k+1}$ divergence-free finite elements on rectangular grids. SIAM J. Numer. Anal. **47**, 2090–2107 (2009)
32. Zhang, S.: On the full $C_1 - Q_k$ finite element spaces on rectangles and cuboids. Adv. Appl. Math. Mech. **2**, 701–721 (2010)
33. Zhang, S.: Quadratic divergence-free finite elements on Powell–Sabin tetrahedral grids. Calcolo **48**(3), 211–244 (2011)